Compositional Modeling of Two-Phase Flow in Porous Media Using Semi-Implicit Scheme

Ondřej Polívka and Jiří Mikyška

***Abstract*—In this paper we deal with the numerical modeling of the compressible two-phase flow of a mixture composed of several components in porous media with species transfer between the phases. We formulate the mathematical model by means of the extended Darcy's laws for all phases, components continuity equations, constitutive relations, and appropriate initial and boundary conditions. The splitting of components among the phases is described by a formulation of the local thermodynamic equilibrium which uses volume, temperature, and moles as specification variables. We solve the problem numerically using a combination of the mixed-hybrid finite element method for the total flux discretization and the finite volume method for the discretization of transport equations, and the semi-implicit time discretization. The proposed numerical flux approximation does not require phase identification and determination of the corresponding phases on adjacent elements. The resulting system of nonlinear algebraic equations is solved by the Newton-Raphson method. In contrast to fully-implicit schemes, the size of the final system does not depend on the number of mixture components.**

***Index Terms*—semi-implicit phase-by-phase upwinding, mixed-hybrid finite element method, finite volume method, constant-volume phase splitting.**

I. Introduction

MATHEMATICAL modeling of gas injection into oil reservoirs is important in dealing with problems like enhanced oil recovery or CO_2 sequestration. The mathematical model has to describe transport of a mixture composed of several chemical components in a porous medium. Depending on the local thermodynamic conditions, the mixture can remain in a single phase or can split into two (or more) phases.

In this paper, we follow our previous work [14], where we have derived a fully-implicit numerical scheme for the compositional modeling in which components splitting among the phases is described by a formulation of the local thermodynamic equilibrium at constant volume, temperature, and moles (VT-flash) [11], [12], [6], [7]. The fully-implicit scheme is stable allowing for long time steps, but it suffers from higher computational costs because a large system of equations has to be solved. Moreover, the size of the final system is proportional to the number of mixture components. A remedy for this disadvantage could be an explicit scheme, where one does not have to solve any system. However, explicit schemes are conditionally stable with very restrictive size of the time step. We propose a semi-implicit approach based on a combination of the mixed-hybrid finite element method (MHFEM) and the finite volume method (FVM). Similarly to the fully-implicit schemes, our method leads to large systems of linear algebraic equations, but it is possible to reduce the size of the final system of equations to a size independent of the number of mixture components. Therefore, the size of the final linear system is significantly reduced which is a desirable feature, especially for mixtures composed of a large number of components.

The paper is structured as follows. In Section II, the mathematical model is formulated by means of partial differential equations representing the conservation laws, Darcy's laws, and by means of the conditions of local thermodynamic equilibrium in the VT-settings. Several fluxes are introduced and some important relations between them are described. Then, the compositional model is formulated and appropriate initial and boundary conditions are prescribed. In Section III, the system of equations is solved numerically using the MHFEM for Darcy's law discretization, and the FVM including upwind technique for the components transport equations discretization. The semi-implicit scheme is derived and linearized using the Newton-Raphson iterative method (NRM), and the system of equations is reduced to a size that is independent of the number of components. In Section IV, the basic steps of the computational algorithm are summarized. Examples of computations using the semi-implicit approach and comparisons of results with the fully-implicit approach are presented in Section V. In Section VI, essential features of the method are commented and some conclusions are drawn. In Appendix, details on the equation of state used in the calculation are provided.

Manuscript received December 31, 2013; revised July 21, 2014. This work was supported by the project P105/11/1507 Development of Computational Models for Simulation of CO2 Sequestration of the Czech Science Foundation and by the project KONTAKT II LH 12064 Computational Methods in Thermodynamics of Hydrocarbon Mixtures of the Ministry of Education, Youth and Sport of the Czech Republic.

O. Polívka is with the Department of Mathematics, Faculty of Nuclear Sciences and Physical Engineering, Czech Technical University in Prague, Trojanova 13, 120 00 Prague 2, Czech Republic, e-mail: ondrej.polivka@fjfi.cvut.cz

J. Mikyška is with the Department of Mathematics, Faculty of Nuclear Sciences and Physical Engineering, Czech Technical University in Prague, Trojanova 13, 120 00 Prague 2, Czech Republic, e-mail: jiri.mikyska@fjfi.cvut.cz

II. Model Equations

A. Transport Equations

Consider two-phase compressible flow of a mixture composed of n_c components in a porous medium with porosity ϕ [-] at a constant temperature T [K]. If we neglect diffusion and capillarity, the transport of the components can be described by the following molar balance equations [10], [14]

$$\frac{\partial(\phi c_i)}{\partial t} + \nabla \cdot \left(\sum_\alpha c_{\alpha,i}\, \mathbf{v}_\alpha \right) = F_i\,, \quad i = 1, \ldots, n_c\,, \quad (1)$$

where $\sum_\alpha$ sums over all phases, c_i is the overall molar concentration of component i [mol m^{-3}], $c_{\alpha,i}$ is the molar concentration of component i in phase α [mol m^{-3}], and F_i is the sink or source term [mol m^{-3}s^{-1}]. The phase velocity

$\mathbf{v}_\alpha$ is given by the extended Darcy's law

$$\mathbf{v}_\alpha = -\lambda_\alpha \mathbf{K}(\nabla p - \varrho_\alpha \mathbf{g}) \,, \quad \lambda_\alpha = \frac{k_{r\alpha}}{\mu_\alpha} \,, \tag{2}$$

where $\mathbf{K} = \mathbf{K}(\mathbf{x})$ is the medium intrinsic permeability [m^2], p is the pressure [Pa], $\varrho_\alpha = \sum_{i=1}^{n_c} c_{\alpha,i} M_i$ is the density of fluid in phase α (M_i is the molar weight of component i [$\mathrm{kg\,mol}^{-1}$]), and $\mathbf{g}$ is the gravitational acceleration vector [$\mathrm{m\,s}^{-2}$]. The α-phase mobility λ_α is given by the ratio of the α-phase relative permeability $k_{r\alpha}$ [-] and α-phase dynamic viscosity μ_α [$\mathrm{kg\,m}^{-1}\mathrm{s}^{-1}$]. The relative permeability and dynamic viscosity depend on properties of phase α as

$$k_{r\alpha} = k_{r\alpha}\left(S_\alpha\right) \,, \quad \mu_\alpha = \mu_\alpha(T, c_{\alpha,1}, \ldots, c_{\alpha,n_c}) \,, \tag{3}$$

where S_α is the saturation of phase α and viscosity is computed using the Lohrenz-Bray-Clark method [9].

B. Phase Computations

As we study generally the two-phase flow, a mixture can stay in the single phase or two phases at each point. To decide on the number of phases from temperature $T > 0$ and overall molar concentrations $c_1, \ldots, c_{n_c}$, we use the constant volume phase stability test described in [12]. In the single-phase case, $c_{\alpha,i} = c_i$, $S_\alpha = 1$ hold, and pressure is given by the Peng-Robinson equation of state (detailed in Appendix) of the form

$$p = p\left(T, c_1, \ldots, c_{n_c}\right). \tag{4}$$

If the VT-stability indicates that the system is in two phases, the splitting of components among the phases is given by the following phase equilibrium conditions [11]

$$\sum_\alpha c_{\alpha,i} S_\alpha = c_i \,, \quad \sum_\alpha S_\alpha = 1 \,, \tag{5a}$$

$$\forall \alpha \neq \beta \,, \ \forall i = 1, \ldots, n_c \,,$$

$$p\left(T, c_{\alpha,1}, \ldots, c_{\alpha,n_c}\right) = p\left(T, c_{\beta,1}, \ldots, c_{\beta,n_c}\right) \,, \tag{5b}$$

$$\widetilde{\mu}_i\left(T, c_{\alpha,1}, \ldots, c_{\alpha,n_c}\right) = \widetilde{\mu}_i\left(T, c_{\beta,1}, \ldots, c_{\beta,n_c}\right) \,. \tag{5c}$$

Equations (5) express the balance of mass and volume (5a), mechanical equilibrium (5b), and chemical equilibrium (5c) in which $\widetilde{\mu}_i$ denotes the chemical potential of component i, which can be derived from the equation of state. The exact form of $\widetilde{\mu}_i$ for the Peng-Robinson equation of state can be found in [6], [11], [12].

The system of $2 \cdot n_c + 2$ equations (5) for unknown molar concentrations of all components in both phases $c_{\alpha,i}$ and phase saturations S_α can be solved by the Newton-Raphson method (for details see [11]). Then, the equilibrium pressure p can be determined using the equation of state as

$$p = p\left(T, c_{\alpha,1}, \ldots, c_{\alpha,n_c}\right), \tag{6}$$

where α is any of the split-phases.

C. Introduction of Fluxes

For the derivation of the numerical scheme, we need to define several fluxes. We denote $\mathbf{q}_{\alpha,i}$ the i-th component flux in phase α, $\mathbf{q}_i$ the i-th component total flux, and $\mathbf{q}$ the total flux given by

$$\mathbf{q}_{\alpha,i} = c_{\alpha,i} \mathbf{v}_\alpha \,, \tag{7a}$$

$$\mathbf{q}_i = \sum_\alpha \mathbf{q}_{\alpha,i} = \sum_\alpha c_{\alpha,i} \mathbf{v}_\alpha \,, \tag{7b}$$

$$\mathbf{q} = \sum_i \mathbf{q}_i = \sum_\alpha c_\alpha \mathbf{v}_\alpha \,, \tag{7c}$$

where $c_\alpha = \sum_{i=1}^{n_c} c_{\alpha,i}$ is the total α-phase concentration. By substituting (2) into (7c), we can formulate Darcy's law for the total flux as

$$\mathbf{q} = -\sum_\alpha c_\alpha \lambda_\alpha \mathbf{K}(\nabla p - \widetilde{\varrho}\mathbf{g}) \,, \tag{8}$$

where

$$\widetilde{\varrho} = \frac{\sum_\alpha c_\alpha \lambda_\alpha \varrho_\alpha}{\sum_\alpha c_\alpha \lambda_\alpha} \tag{9}$$

is an average density. Then, using (7a), (8), and (2), $\mathbf{q}_{\alpha,i}$ can be evaluated as

$$\mathbf{q}_{\alpha,i} = \frac{c_{\alpha,i}\lambda_\alpha}{\sum_\beta c_\beta \lambda_\beta} \left(\mathbf{q} - \sum_\beta c_\beta \lambda_\beta \left(\varrho_\beta - \varrho_\alpha\right) \mathbf{K}\mathbf{g} \right) \,, \tag{10}$$

and, consequently, the total component flux is given from (7b) as

$$\mathbf{q}_i = \sum_\alpha \frac{c_{\alpha,i}\lambda_\alpha}{\sum_\beta c_\beta \lambda_\beta} \left(\mathbf{q} - \sum_\beta c_\beta \lambda_\beta \left(\varrho_\beta - \varrho_\alpha\right) \mathbf{K}\mathbf{g} \right) \,. \tag{11}$$

D. Mathematical Formulation

Let $\Omega \subset \mathbb{R}^d$ ($d \in \mathbb{N}$) be a bounded domain and I be a time interval. In $\Omega \times I$, we solve for $c_i = c_i(\mathbf{x}, t)$ the following equations which can be obtained from the transport equations (1) and (7b)

$$\frac{\partial(\phi c_i)}{\partial t} + \nabla \cdot \mathbf{q}_i = F_i \,, \quad i = 1, \ldots, n_c \,, \tag{12}$$

where $\mathbf{q}_i$ is given by (11), and $\mathbf{q}$ is given by (8). The molar concentrations $c_{\alpha,i}$ and saturations are related to the overall molar concentrations c_i by (5) from which we also determine the pressure (see Section II-B). Relative permeabilities and viscosities are given by (3). For this system of equations, we impose the following initial and boundary conditions

$$c_i(\mathbf{x}, 0) = c_i^0(\mathbf{x}) \,, \quad \mathbf{x} \in \Omega \,, \ i = 1, \ldots, n_c \,, \tag{13a}$$

$$p(\mathbf{x}, t) = p^D(\mathbf{x}, t) \,, \quad \mathbf{x} \in \Gamma_p \,, \ t \in I \,, \tag{13b}$$

$$\mathbf{q}_i(\mathbf{x}, t) \cdot \mathbf{n}(\mathbf{x}) = 0 \,, \quad \mathbf{x} \in \Gamma_q \,, \ t \in I \,, \ i = 1, \ldots, n_c \,, \tag{13c}$$

where $\mathbf{n}$ is the unit outward normal vector to the boundary $\partial\Omega$, $\Gamma_p \cup \Gamma_q = \partial\Omega$, and $\Gamma_p \cap \Gamma_q = \emptyset$. Initial values of molar concentrations are given by (13a), whereas (13b) is the Dirichlet boundary condition prescribing the pressure p_D on Γ_p, and (13c) is the zero Neumann boundary condition representing impermeable boundary on Γ_q. We assume that Γ_p is the outflow boundary, so no boundary condition for concentration has to be imposed.

III. Numerical Model

The system of equations (12), (5), and (13) is solved numerically using a combination of the MHFEM for the total flux discretization, and the FVM for the transport equations discretization. The obtained system is linearized by the NRM. The number of phases is determined locally on every element using the stability algorithm described in [12] at constant temperature and overall molar concentrations. In two-phase elements, the splitting of components among the phases is computed from the VT-flash algorithm [11]. Once the phase splitting is computed, pressure is evaluated readily using the equation of state.

We consider a 2D polygonal domain Ω with the boundary $\partial\Omega$ which is covered by a conforming triangulation $\mathcal{T}_\Omega$. We denote K the element of the mesh $\mathcal{T}_\Omega$ with area $|K|$, E the edge of an element with the length $|E|$, n_k the number of elements of the triangulation, and n_e the number of edges of the mesh.

A. Discretization of Darcy's Law for the Total Flux

The total flux $\mathbf{q}$ is approximated locally in the Raviart-Thomas space of the lowest order ($\mathrm{RT}_0(K)$) over the element $K \in \mathcal{T}_\Omega$ [2], [14], [10] as

$$\mathbf{q}|_K = \sum_{E\in\partial K} q_{K,E}\mathbf{w}_{K,E}\,, \tag{14}$$

where the coefficient $q_{K,E}$ represents the numerical flux of vector function $\mathbf{q}$ through the edge E on the element K with respect to the outer normal, and $\mathbf{w}_{K,E}$ is the basis function of $\mathrm{RT}_0(K)$ associated with the edge E. The basis functions are given by

$$\mathbf{w}_{K,E}(\mathbf{x}) = \frac{1}{2|K|}\left(\mathbf{x}-\mathbf{N}_{K,E}\right), \quad \forall \mathbf{x}\in K\,,\ E\in\partial K\,, \tag{15}$$

where $\mathbf{N}_{K,E} \in K$ is a node against edge E. The basis functions (15) satisfy the following properties

$$\nabla\cdot\mathbf{w}_{K,E}(\mathbf{x}) = \frac{1}{|K|}\,, \quad \mathbf{w}_{K,E}(\mathbf{x})\cdot\mathbf{n}_{K,E'} = \frac{\delta_{E,E'}}{|E|}\,. \tag{16}$$

Using (16) and techniques described in [14], we derive the mixed-hybrid finite element discretization of Darcy's law for the total flux (8) as

$$q_{K,E} = \sum_{\alpha\in\Pi(K)} c_{\alpha,K}\lambda_{\alpha,K}\left(\alpha_E^K p_K - \right.$$
$$\left. - \sum_{E'\in\partial K}\beta_{E,E'}^K\widehat{p}_{K,E'} + \gamma_E^K\widetilde{\varrho}_K\right), \quad E\in\partial K, \tag{17}$$

where the coefficients are given by

$$\alpha_E^K = \sum_{E'\in\partial K} A^{-1}_{K,E,E'}\,, \quad \beta^K_{E,E'} = A^{-1}_{K,E,E'}\,,$$
$$\gamma_E^K = \sum_{E'\in\partial K} A^{-1}_{K,E,E'}G_{K,E'}\,, \tag{18}$$

where $A^{-1}_{K,E,E'}$ is an element of the inverse matrix $\mathbf{A}_K^{-1}$, $\mathbf{A}_K = \left(A_{K,E,E'}\right)_{E,E'\in\partial K}$, and

$$A_{K,E,E'} = \int_K \mathbf{K}^{-1}\mathbf{w}_{K,E}\cdot\mathbf{w}_{K,E'}\,,\ G_{K,E'} = \int_K \mathbf{g}\cdot\mathbf{w}_{K,E'}\,. \tag{19}$$

In (17), $\Pi(K)$ is set of all phases on element K, p_K denotes the cell pressure average, $\widehat{p}_{K,E'}$ is the edge pressure average, $c_{\alpha,K}$, $\lambda_{\alpha,K}$, $\widetilde{\varrho}_K$ are the mean values of concentration and mobility of phase α, and average density on element K. The cell-averaged quantities are functions of the overall molar concentrations and temperature at element K; their evaluation is described in Section III-C.

In the mixed-hybrid formulation, we require the continuity of total flux normal component and pressure on the edge E between neighboring elements $K, K' \in \mathcal{T}_\Omega$ which can be formulated as

$$q_{K,E} + q_{K',E} = 0\,, \tag{20}$$
$$\widehat{p}_{K,E} = \widehat{p}_{K',E} =: \widehat{p}_E\,. \tag{21}$$

The boundary conditions (13b), (13c) are discretized as

$$\widehat{p}_E = p^D(E)\,, \quad \forall E\subset\Gamma_p\,, \tag{22a}$$
$$q_{K,E} = 0\,, \quad \forall E, K : E\subset\Gamma_q, E\in\partial K\,, \tag{22b}$$

where $p^D(E)$ is the prescribed value of pressure p^D averaged on the edge E.

We can eliminate the numerical flux $q_{K,E}$ by substituting from (17) into (20) and (22b). For further derivation, let us consider time dependent quantities at time t_{n+1} denoted by upper index $n+1$. Then, Equations (17)–(22) transform to the following system of n_e linear algebraic equations $\mathcal{F}_E = 0$, where

$$\mathcal{F}_E = \begin{cases} \sum\limits_{K:E\in\partial K}\left(\sum\limits_{\alpha\in\Pi(K)} c^{n+1}_{\alpha,K}\lambda^{n+1}_{\alpha,K}\right)\Big(\alpha_E^K p_K^{n+1} - \\ - \sum\limits_{E'\in\partial K}\beta^K_{E,E'}\widehat{p}^{\,n+1}_{E'} + \gamma_E^K\widetilde{\varrho}_K^{n+1}\Big)\,, \quad \forall E\not\subset\Gamma_p\,, \\ \widehat{p}_E^{n+1} - p^D(E)\,, \quad \forall E\subset\Gamma_p\,. \end{cases} \tag{23}$$

Herein, the symbol $\sum_{K:E\in\partial K}$ denotes the sum over the elements adjacent to the edge E.

B. Discretization of the Transport Equations

For the discretization of the transport equations (12) with the initial and boundary conditions (13), similarly as in [14], we use the FVM [8]. Unlike in [14], where the fully-implicit scheme was derived, here, we derive the semi-implicit scheme. Integrating (12) over an arbitrary element $K\in\mathcal{T}_\Omega$ and using Green's theorem, we have

$$\frac{\mathrm{d}}{\mathrm{d}t}\int_K \phi(\mathbf{x})c_i(\mathbf{x},t) + \int_{\partial K}\mathbf{q}_i(\mathbf{x},t)\cdot\mathbf{n}_{\partial K}(\mathbf{x}) = \int_K F_i(\mathbf{x})\,,$$
$$i = 1,\ldots,n_c\,. \tag{24}$$

Applying the mean value theorem on (24), and denoting $\phi_K, c_{i,K}, F_{i,K}$, the averaged values of ϕ, c_i, F_i $(i=1,\ldots,n_c)$ over the cell K, respectively, the semi-discrete form of (12) reads as

$$\frac{\mathrm{d}(\phi_K c_{i,K})}{\mathrm{d}t}|K| + \sum_{E\in\partial K} q_{i,K,E} = F_{i,K}|K|\,, \tag{25}$$

where $q_{i,K,E}$ is a numerical approximation of $\int_E \mathbf{q}_i\cdot\mathbf{n}_{K,E}$ for $E\in\partial K$. To evaluate the numerical flux $q_{i,K,E}$, we

propose the following upwind technique

$$q_{i,K,E} = \begin{cases} \sum\limits_{\alpha\in\Pi(K,E)^+} q_{\alpha,i,K,E} - \sum\limits_{\beta\in\Pi(K',E)^+} q_{\beta,i,K',E}\,, \\ \qquad\qquad\qquad\qquad \forall E \notin \partial\Omega\,, \\ \sum\limits_{\alpha\in\Pi(K,E)^+} q_{\alpha,i,K,E}\,, \quad \forall E \in \Gamma_p\,, \\ 0\,, \quad \forall E \in \Gamma_q\,, \end{cases} \tag{26}$$

where $\Pi(K,E)^+ = \{\alpha \in \Pi(K) \,|\, q_{\alpha,i,K,E} > 0\}$ for $E \in \partial K$, and $q_{\alpha,i,K,E}$ is given by

$$q_{\alpha,i,K,E} = \frac{c_{\alpha,i,K}\,\lambda_{\alpha,K}}{\sum\limits_{\beta\in\Pi(K)} c_{\beta,K}\,\lambda_{\beta,K}}\,(q_{K,E} - \\ - \sum_{\beta\in\Pi(K)} c_{\beta,K}\,\lambda_{\beta,K}\,(\varrho_{\beta,K} - \varrho_{\alpha,K})\,\gamma_E^K\Big)\,. \tag{27}$$

Notice that (26) is an approximation of (11), and (27) is a discrete form of (10). In (26), we sum only over the outflowing phases through the edge E. This method ensures that no phase identification or phase interconnection between neighboring elements is necessary, and the total component fluxes are balanced on each inner edge. In (27) $q_{K,E}$ is given by (17), $c_{\alpha,i,K}$ and $S_{\alpha,K}$ are computed locally on each element by VT-flash (see Section II-B), and from them, $c_{\alpha,K}$, $\lambda_{\alpha,K}$, and $\varrho_{\alpha,K}$ are evaluated.

Assuming that the porosity does not depend on time, the time derivative of $c_{i,K}$ in (25) is approximated by the time difference with a time step Δt_n. For every n, all $K \in \mathcal{T}_\Omega$, and $i = 1,\dots,n_c$ the semi-implicit scheme can be derived from Equation (25) in a form $\mathcal{F}_{K,i} = 0$, where

$$\mathcal{F}_{K,i} = \phi_K|K|\frac{c_{i,K}^{n+1} - c_{i,K}^{n}}{\Delta t_n} + \sum_{E\in\partial K} q_{i,K,E}^{n+1/2} - F_{i,K}|K|\,, \tag{28}$$

where $q_{i,K,E}^{n+1/2}$ is given by (26) using

$$q_{\alpha,i,K,E}^{n+1/2} = \frac{c_{\alpha,i,K}^{n}\,\lambda_{\alpha,K}^{n}}{\sum\limits_{\beta\in\Pi(K)^n} c_{\beta,K}^{n}\,\lambda_{\beta,K}^{n}}\,\Big(q_{K,E}^{n+1} - \\ - \sum_{\beta\in\Pi(K)^n} c_{\beta,K}^{n}\,\lambda_{\beta,K}^{n}\,\big(\varrho_{\beta,K}^{n} - \varrho_{\alpha,K}^{n}\big)\,\gamma_E^K\Big)\,. \tag{29}$$

Note that only $q_{K,E}^{n+1}$ is taken from the new time level in (29), all other terms are given explicitly from the previous time level including $\Pi(K)^n$ which denotes phases on element K at time level n. This is the key point enabling to reduce the system of equations to a size that is independent of the number of mixture components described in the next section.

The initial conditions (13a) are approximated as

$$c_{i,K}^0 = c_i^0(K)\,, \quad \forall K \in \mathcal{T}_\Omega\,,\ i = 1,\dots,n_c\,, \tag{30}$$

where $c_i^0(K)$ denotes the average value of c_i^0 on element K.

C. Assembling the Final System

In Equations (23) and (28), we have denoted $\mathcal{F}_E$ and $\mathcal{F}_{K,i}$, (for the edge $E \in \{1,\dots,n_e\}$, element $K \in \{1,\dots,n_k\}$, and component $i \in \{1,\dots,n_c\}$) the expressions which represent the components of a vector $\boldsymbol{\mathcal{F}}$. To evaluate quantities $c_{\alpha,K}$, $\lambda_{\alpha,K}$, $\widetilde{\varrho}_K$ contained in (23) and also other element-averaged functions depending on the phase splitting, we perform VT-flash calculation on element K using the cell-averaged values $c_{1,K}^{n+1},\dots,c_{n_c,K}^{n+1}$ and temperature T. The cell-averaged pressure p_K^{n+1} is also given implicitly by the result of the VT-flash and by (6) as

$$p_K^{n+1} = p\left(T, c_{\alpha,1,K}^{n+1},\dots,c_{\alpha,n_c,K}^{n+1}\right). \tag{31}$$

This relation is valid in both single- and two-phase states due to (5b). We therefore solve a nonlinear system of algebraic equations of $n_k\cdot n_c + n_e$ equations

$$\begin{aligned} \boldsymbol{\mathcal{F}}_1 &= [\mathcal{F}_{1,1}\,,\dots,\mathcal{F}_{n_k,n_c}]^T = \mathbf{0} \\ \boldsymbol{\mathcal{F}}_2 &= [\mathcal{F}_1\,,\dots,\mathcal{F}_{n_e}]^T = \mathbf{0} \end{aligned} \tag{32}$$

for unknown primary variables – overall molar concentrations $c_{1,K}^{n+1},\dots,c_{n_c,K}^{n+1}$, $K \in \{1,\dots,n_k\}$, and pressures on the edges $\widehat{p}_E^{n+1}$, $E \in \{1,\dots,n_e\}$.

To solve (32), we use the NRM [16]. In each iteration of the NRM, we need to solve the following system of linear algebraic equations

$$\begin{bmatrix} \mathbf{J}_{11} & \mathbf{J}_{12} \\ \mathbf{J}_{21} & \mathbf{J}_{22} \end{bmatrix} \begin{bmatrix} \boldsymbol{\delta c} \\ \boldsymbol{\delta \widehat{p}} \end{bmatrix} = \begin{bmatrix} -\boldsymbol{\mathcal{F}}_1 \\ -\boldsymbol{\mathcal{F}}_2 \end{bmatrix}. \tag{33}$$

The Jacobian matrix of system (33) composed of blocks $\mathbf{J}_{11},\dots,\mathbf{J}_{22}$ is sparse and nonsymmetric. Elements of the matrix can be evaluated analytically using the following relations

$$\begin{aligned} (\mathbf{J}_{11})_{K,i;K',j} &= \frac{\partial \mathcal{F}_{K,i}}{\partial c_{j,K'}^{n+1}}\,, \qquad (\mathbf{J}_{12})_{K,i;E} = \frac{\partial \mathcal{F}_{K,i}}{\partial \widehat{p}_E^{n+1}}\,, \\ (\mathbf{J}_{21})_{E;K,j} &= \frac{\partial \mathcal{F}_E}{\partial c_{j,K}^{n+1}}\,, \qquad (\mathbf{J}_{22})_{E,E'} = \frac{\partial \mathcal{F}_E}{\partial \widehat{p}_{E'}^{n+1}}\,, \end{aligned} \tag{34}$$

where $i,j = 1,\dots,n_c$; $K,K' = 1,\dots,n_k$; $E,E' = 1,\dots,n_e$. The vectors of solutions $\boldsymbol{\delta c}$ and $\boldsymbol{\delta \widehat{p}}$ contain the corrections of $n_k\cdot n_c$ molar concentrations $\delta c_{i,K}^{n+1}$ and n_e pressures on the edges $\delta \widehat{p}_E^{n+1}$, which are computed in each NRM-iteration and added to the values of $c_{i,K}^{n+1}$ and $\widehat{p}_E^{n+1}$ given from the previous iteration. The iteration procedure ends when the condition

$$\|\boldsymbol{\mathcal{F}}\| < \varepsilon \tag{35}$$

is satisfied for a chosen $\varepsilon > 0$ [16].

The proposed semi-implicit scheme allows to reduce the size of system (33). By evaluating $q_{K',E}$ from (20) and substituting it into $q_{\beta,i,K',E}$ in (26), matrix $\mathbf{J}_{11}$ becomes block-diagonal, each block being a $n_c \times n_c$ matrix corresponding to a single element. Then, by inverting the diagonal blocks, $\mathbf{J}_{21}$ can be eliminated and (33) transforms to

$$\begin{bmatrix} \mathbf{J}_{11} & \mathbf{J}_{12} \\ \mathbf{0} & \mathbf{J}_{22} - \mathbf{J}_{21}\,(\mathbf{J}_{11})^{-1}\,\mathbf{J}_{12} \end{bmatrix} \begin{bmatrix} \boldsymbol{\delta c} \\ \boldsymbol{\delta \widehat{p}} \end{bmatrix} = \\ = \begin{bmatrix} -\boldsymbol{\mathcal{F}}_1 \\ \mathbf{J}_{21}\,(\mathbf{J}_{11})^{-1}\,\boldsymbol{\mathcal{F}}_1 - \boldsymbol{\mathcal{F}}_2 \end{bmatrix}. \tag{36}$$

Then, the system can be reduced to the final system

$$\Big[\mathbf{J}_{22} - \mathbf{J}_{21}\,(\mathbf{J}_{11})^{-1}\,\mathbf{J}_{12}\Big]\,\boldsymbol{\delta \widehat{p}} = \\ = \mathbf{J}_{21}\,(\mathbf{J}_{11})^{-1}\,\boldsymbol{\mathcal{F}}_1 - \boldsymbol{\mathcal{F}}_2\,, \tag{37}$$

for unknowns $\delta\widehat{p}_E^{n+1}$, $E = 1, \ldots, n_e$. Thus, we eliminated the internal degrees of freedom $\delta c_{i,K}^{n+1}$, $i = 1, \ldots, n_c$, $K = 1, \ldots, n_k$, which are subsequently computed from (36) using the evaluated inversion of $\mathbf{J}_{11}$ as

$$\boldsymbol{\delta c} = -\left(\mathbf{J}_{11}\right)^{-1}\left(\boldsymbol{\mathcal{F}}_1 + \mathbf{J}_{12}\boldsymbol{\delta}\widehat{\boldsymbol{p}}\right). \tag{38}$$

The procedure of reducing the system in (33) to (37) is similar to static condensation described in [2]. The inversion of $\mathbf{J}_{11}$ is possible since the matrix is diagonally dominant for small time steps, and can be computed in parallel by inverting diagonal blocks in $\mathbf{J}_{11}$.

The robustness of the NRM is increased by using the line-search technique [16] which ensures decreasing of $\|\boldsymbol{\mathcal{F}}\|$ in each NRM-iteration with respect to the previous iteration. If the NRM cannot converge in 20 iterations, the time step is restarted and the value Δt_n is halved. If the NRM converges in less than 5 iterations, the time step is accepted and the next time step size is increased ($\Delta t_{n+1} = 1.2\Delta t_n$).

In contrast to the fully-implicit approach in [14], where it was necessary to solve a system of size $(n_c \cdot n_K + n_E) \times (n_c \cdot n_K + n_E)$ as in (33), here in the semi-implicit approach, the size of the final system (37) is $n_E \times n_E$, which does not depend on the number of mixture components. The linearization is performed with respect to the persistent variables – i.e. well defined independently of whether a given element is in a single phase or two phases. The derivatives in (34) are also well defined in both single phase and two phases. Therefore, our schemes here and in [14] perform well in both cases and no primary variables switching is needed for treating phase appearance/disappearance (cf. [3], [4], [15]). As the discretization of the transport equations is based on the approximation of the total component flux, the connection between the elements with different number of phases is treated in a natural way.

IV. Algorithm

The computation proceeds in the following steps:

1) Initialize the geometry, physical and chemical parameters, and molar concentrations, generate a domain triangulation. Compute α_E^K, $\beta_{E,E'}^K$, and γ_E^K for all elements and their edges.
2) Calculate pressures p_K on each element using the equation of state (4) and initial molar concentrations, then initialize all edge pressures $\widehat{p}_E$ by averaging p_K on neighboring elements.
3) Repeat until the predetermined final time is reached ($t_n \in I$):
   a) Repeat the NRM-iterations until the convergence criterion (35) is satisfied:
      i) Perform the stability and flash calculations (see Section II-B) to obtain a number of phases and their compositions locally on all elements.
      ii) For each K, compute the cell-averaged pressures p_K^{n+1} using (31), and average densities $\widetilde{\varrho}_K^{n+1}$ using (9).
      iii) Evaluate the total fluxes $q_{K,E}^{n+1}$ using (17), and phase fluxes $q_{\alpha,i,K,E}^{n+1/2}$ using (29) and the quantities from the previous time step.
      iv) Assemble and solve system (37) for corrections of pressures $\delta\widehat{p}_E^{n+1}$.
      v) From (38) compute corrections of molar concentrations $\delta c_{i,K}^{n+1}$ using $\mathbf{J}_{11}^{-1}$ computed in the previous step.
      vi) Add corrections $\delta c_{i,K}^{n+1}$ and $\delta\widehat{p}_E^{n+1}$ to $c_{i,K}^{n+1}$ and $\widehat{p}_E^{n+1}$, respectively, check the convergence criterion (35).
   b) Evaluate $\lambda_{\alpha,K}^{n+1}$ and $\varrho_{\alpha,K}^{n+1}$ on each element for all present phases.
   c) Continue to the next time level ($n \to n+1$).

In step 2), only single phase is considered. In steps i. and ii., number of phases, their compositions, and p_K^{n+1} are computed using the data from the last available Newton iteration. In the first iteration, data from the previous time step are used.

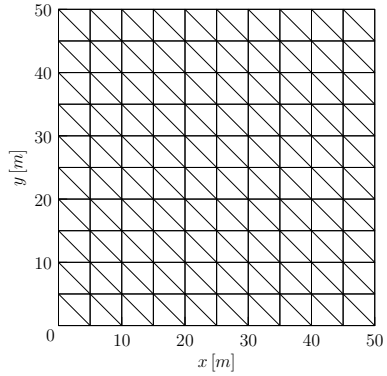

Fig. 1. Structure of the computational grid.

V. Results

In this section, we present numerical results of compositional simulations of carbon dioxide (CO_2) injection into reservoirs filled with different mixtures at constant temperature. The results have been computed using the numerical scheme described in Section III. We have computed the flow in a 2D square reservoir $50 \times 50\,\mathrm{m}^2$ with porosity $\phi = 0.2$ and isotropic permeability $\mathbf{K} = k = 9.87 \cdot 10^{-15}\,\mathrm{m}^2$ (i.e. 10 mD). Structure of the computational grid consisting of 200 elements is shown in Fig. 1. Parameter ε from the NRM-convergence criterion (35) has been chosen 10^{-6} for all computations. The systems of linear algebraic equations have been solved using the direct solver UMFPACK [17], [18], [19], [20]. All examples have been computed on a grid of 3200 elements. In each figure, isolines of the overall molar fraction $c_i/(\sum_{i=1}^{n_c} c_i)$ are depicted, and the two-phase region is represented by gray color. We also mention the average time steps (computed as arithmetic mean from 5 values at time levels: 0.32, 0.63, 0.95, 1.27, and 1.58 years) and CPU times using the current scheme and the fully-implicit scheme [14] in every example. All simulations have been computed on Six-Core AMD Opteron(tm) Processor 2427 at 2.2 GHz and 32 GB memory. Only VT-flash calculations were performed in parallel. The rest of the computation was sequential.

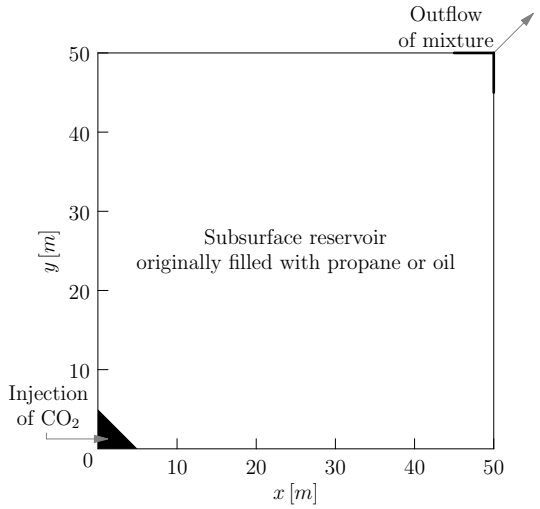

Fig. 2. Outline of the simulated reservoir.

TABLE I
RELEVANT PARAMETERS OF THE PENG-ROBINSON EQUATION OF STATE (40) FOR EXAMPLES 1 AND 2. VOLUME TRANSLATION IS NOT USED.

i (component)	p_{ci} [MPa]	T_{ci} [K]	V_{ci} [m^{3}mol^{-1}]
1 (CO_2)	7.375	304.14	$9.416 \cdot 10^{-5}$
2 (C_3)	4.248	369.83	$2 \cdot 10^{-4}$

i (component)	M_i [g mol^{-1}]	ω_i [-]	δ_{i1} [-]	δ_{i2} [-]
1 (CO_2)	44	0.239	0	0.15
2 (C_3)	44.0962	0.153	0.15	0

A. Injection of Carbon Dioxide into Propane Reservoir

Let us consider a cut through a reservoir filled with liquid propane (C_3) at initial pressure $p = 2.5$ MPa and temperature $T = 311$ K. In the left bottom corner of the reservoir, gaseous CO_2 is injected, and in the right upper corner, the mixture of CO_2 and propane is produced (Fig. 2). The injection rate of CO_2 is 1778.1 mol/day. The parameters of the Peng-Robinson equation of state for both components of the mixture are summarized in Table I. In these settings, both CO_2 and propane are single-phase but when mixed, the mixture can split into two phases. The boundary of the domain is impermeable except for the outflow corner where pressure $p = 2.5$ MPa is maintained. Relative permeability depends linearly on saturation as $k_{r\alpha}(S_\alpha) = S_\alpha$ for each phase α.

Example 1: In Fig. 3, a simulation of CO_2 injection into a horizontal reservoir originally filled with propane is shown at four different times. Isolines of CO_2 overall molar fraction are distributed uniformly between the two displayed values of 0.9 and 0.1. The mixture stays in the single phase in the majority of the domain, only in the zone where the molar fractions are greater than 0.1 and less than 0.9, the two-phase region (colored in gray) appears. In comparison with results of the fully-implicit scheme [14], the contours of CO_2 overall molar fraction are almost the same. The average time step is 153 minutes for the semi-implicit scheme and 179 minutes for the fully-implicit scheme. The computation to $t = 1.58$ years lasted 8.9 hours using the semi-implicit scheme and 9.4 hours using the fully-implicit scheme.

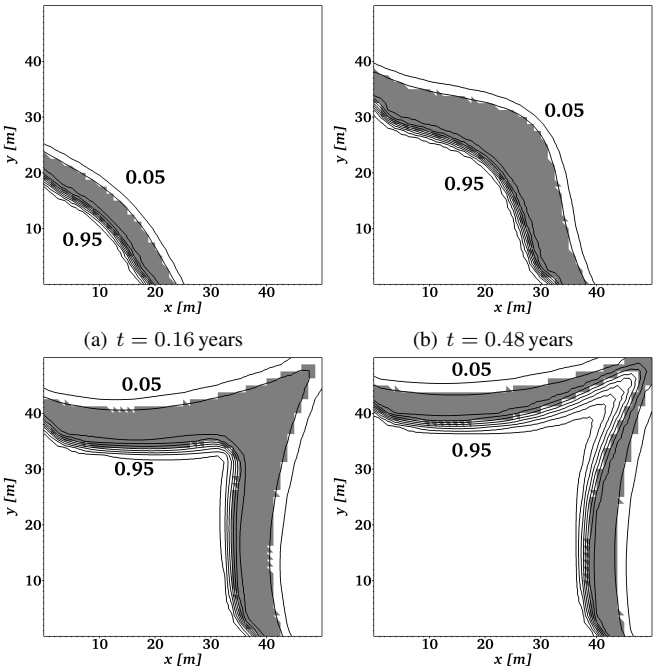

(a) $t = 0.16$ years (b) $t = 0.48$ years

(c) $t = 0.79$ years (d) $t = 1.11$ years

Fig. 3. Isolines of CO_2 overall molar fraction and the two-phase region (gray color) at different times. Contours are distributed uniformly between the two printed values. The solution is computed on a grid of 3200 elements: Example 1.

Example 2: In this example, we simulate the CO_2 injection into a vertical propane reservoir. So the only difference between this and the previous example is the non-zero gravity here. Uniformly distributed contours of CO_2 overall molar fraction between 0.9 and 0.1 are visualized in Fig. 4. The single-phase mixture occupies a major part of the domain during the simulation but in the mixing zone a two-phase domain also develops. At time $t = 0.55$ years, we observed the maximum number of two-phase elements during the whole simulation. Afterwards, the number of two-phase elements decreases. In comparison with the fully-implicit scheme [14], the results almost coincide, and the average time steps are 141 minutes (the current scheme) and 280 minutes (the fully-implicit scheme). The computation to $t = 1.58$ years lasted 51.6 hours using the semi-implicit scheme and 10.4 hours using the fully-implicit scheme.

B. Injection of Carbon Dioxide into Oil Reservoir

Let us consider a cut through an oil (8-component hydrocarbon mixture) reservoir at initial pressure $p = 2.76$ MPa and temperature $T = 403.15$ K. The initial overall molar fractions of the oil components in the reservoir are written in Table II. Gaseous CO_2 is injected in the left bottom corner of the reservoir, and the mixture of CO_2 and oil is produced in the right upper corner. The injection rate of CO_2 is 5578.2 mol/day. The reservoir is outlined in Fig. 2. The parameters of the Peng-Robinson equation of state for all components of the mixture are summarized in Table III. In these settings, the mixture can stay in the single phase or two phases. The boundary of the domain is impermeable except for the outflow corner where pressure $p = 2.76$ MPa is maintained. Relative permeability depends quadratically on saturation as $k_{r\alpha}(S_\alpha) = S_\alpha^2$ for each phase α.

TABLE III
RELEVANT PARAMETERS OF THE PENG-ROBINSON EQUATION OF STATE (40) FOR EXAMPLES 3 AND 4. VOLUME TRANSLATION IS NOT USED.

i (component)	p_{c_i} [MPa]	T_{ci} [K]	V_{ci} [$m^3 mol^{-1}$]	M_i [$g\,mol^{-1}$]	ω_i [-]
1 (CO_2)	7.375	304.14	$9.416 \cdot 10^{-5}$	44	0.239
2 (N_2)	3.39	126.21	$8.988 \cdot 10^{-5}$	28	0.039
3 (C_1)	4.599	190.56	$9.84 \cdot 10^{-5}$	16	0.011
4 (C_2–C_3)	4.654	327.81	$1.6571 \cdot 10^{-4}$	34.96	0.11783
5 (C_4–C_5)	3.609	435.62	$2.7522 \cdot 10^{-4}$	62.98	0.21032
6 (C_6–C_{10})	2.504	574.42	$4.6839 \cdot 10^{-4}$	110.21	0.41752
7 (C_{11}–C_{24})	1.502	708.95	$9.3876 \cdot 10^{-4}$	211.91	0.66317
8 (C_{25+})	0.76	891.47	$1.9298 \cdot 10^{-3}$	462.79	1.7276

i (component)	δ_{i1} [-]	δ_{i2} [-]	δ_{i3} [-]	δ_{i4} [-]	δ_{i5} [-]	δ_{i6} [-]	δ_{i7} [-]	δ_{i8} [-]
1 (CO_2)	0	0	0.15	0.15	0.15	0.15	0.15	0.08
2 (N_2)	0	0	0.1	0.1	0.1	0.1	0.1	0.1
3 (C_1)	0.15	0.1	0	0.0346	0.0392	0.0469	0.0635	0.1052
4 (C_2–C_3)	0.15	0.1	0.0346	0	0	0	0	0
5 (C_4–C_5)	0.15	0.1	0.0392	0	0	0	0	0
6 (C_6–C_{10})	0.15	0.1	0.0469	0	0	0	0	0
7 (C_{11}–C_{24})	0.15	0.1	0.0635	0	0	0	0	0
8 (C_{25+})	0.08	0.1	0.1052	0	0	0	0	0

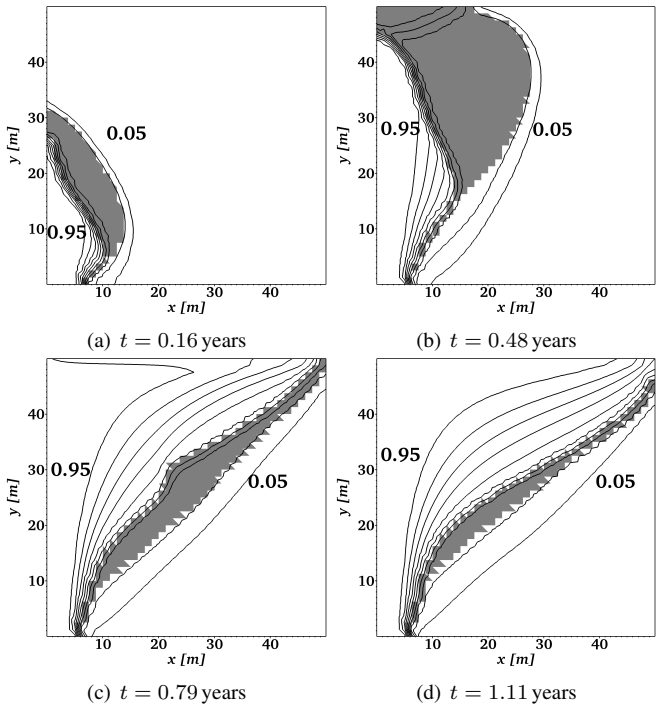

(a) $t = 0.16$ years (b) $t = 0.48$ years

(c) $t = 0.79$ years (d) $t = 1.11$ years

Fig. 4. Isolines of CO_2 overall molar fraction and the two-phase region (gray color) at different times. Contours are distributed uniformly between the two printed values. The solution is computed on a grid of 3200 elements: Example 2.

Example 3: In Fig. 5, a simulation of CO_2 injection in the left bottom corner of a horizontal reservoir originally filled with oil is shown. In the right upper corner, the mixture is produced. In each of the 8 plots, isolines of the overall molar fractions are visualized for every component at time $t = 1.36$ years. Contours are distributed uniformly between the displayed values. In each figure the two-phase region is colored in gray color. In comparison with Examples 1 and 2, the two-phase region occupies a major part of the domain (not only the part between 0.9 and 0.1 contours of CO_2 molar fraction). If we compare the simulations from the semi-implicit and fully-implicit schemes, we obtain almost identical results. We have measured the average time step 133 minutes and 347 minutes for the semi-implicit and fully-implicit schemes, respectively. The computation to $t = 1.58$ years lasted 70.9 hours using the semi-implicit scheme and 66.9 hours using the fully-implicit scheme.

TABLE II
THE INITIAL OVERALL MOLAR FRACTIONS IN THE RESERVOIR FOR EXAMPLES 3 AND 4.

Component	CO_2	N_2	C_1	C_2–C_3
Overall molar fraction	0.0086	0.0028	0.4451	0.1207
Component	C_4–C_5	C_6–C_{10}	C_{11}–C_{24}	C_{25+}
Overall molar fraction	0.0505	0.1328	0.1660	0.0735

Example 4: This example is similar to Example 3, but this time we simulate injection of CO_2 into a vertical oil reservoir. CO_2 is injected in the left bottom corner and the mixture is produced in the right upper corner. Results of the simulation at time $t = 1.36$ years are shown in Fig. 6 using the isolines of the overall molar fractions of each component. The two-phase region is colored in gray in each figure. As in Example 3, also here, the two-phase region occupies a significant part of the reservoir. The semi-implicit scheme with the average time step of 126 minutes has given similar

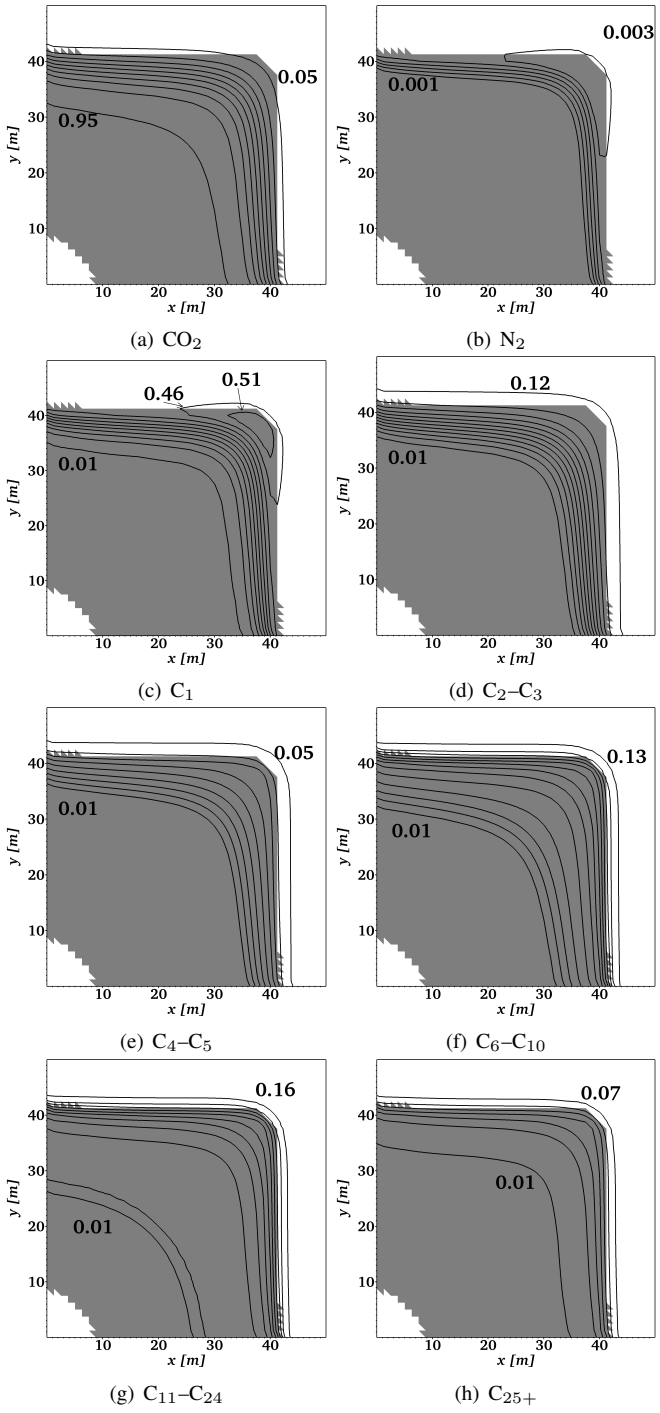

(a) CO_2 (b) N_2 (c) C_1 (d) C_2–C_3 (e) C_4–C_5 (f) C_6–C_{10} (g) C_{11}–C_{24} (h) C_{25+}

Fig. 5. Isolines of the overall molar fractions and the two-phase region (gray color) at $t = 1.36$ years. Contours are distributed uniformly between the two printed values. The solution is computed on a grid of 3200 elements: Example 3.

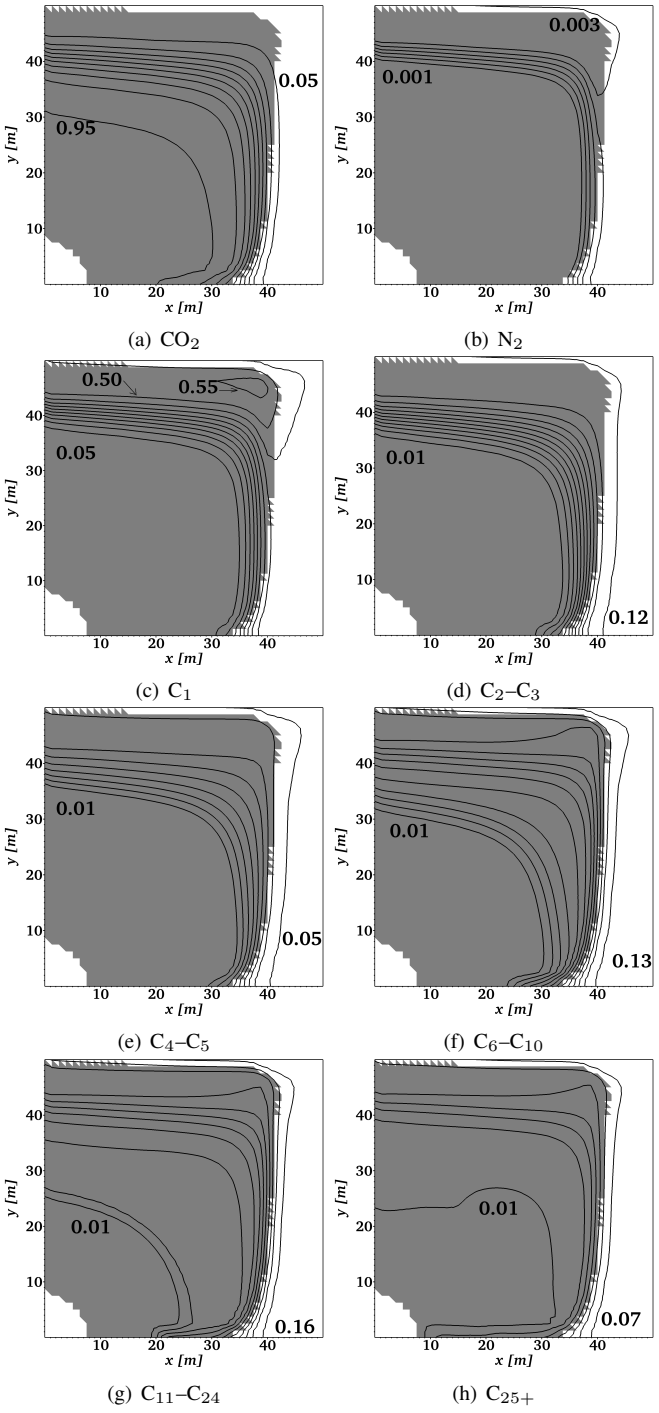

(a) CO_2 (b) N_2 (c) C_1 (d) C_2–C_3 (e) C_4–C_5 (f) C_6–C_{10} (g) C_{11}–C_{24} (h) C_{25+}

Fig. 6. Isolines of the overall molar fractions and the two-phase region (gray color) at $t = 1.36$ years. Contours are distributed uniformly between the two printed values. The solution is computed on a grid of 3200 elements: Example 4.

results as the fully-implicit scheme with the average time step of 233 minutes. The computation to $t = 1.58$ years lasted 96.9 hours using the semi-implicit scheme and 106.5 hours using the fully-implicit scheme.

VI. Conclusion

We have developed a compositional model for the reservoir simulation based on the semi-implicit time discretization. Unlike the fully-implicit approach derived in [14] the method proposed in this paper makes it possible to reduce the resulting system of equations to a size that does not depend on the number of mixture components. This advantageous feature is especially important for simulations involving mixtures with many components. Numerical experiments indicate that the results computed using the semi-implicit and fully-implicit schemes match each other very well. Although the semi-implicit scheme enforces smaller time steps in comparison with the fully-implicit scheme, the time steps are much larger than those allowed by the explicit scheme. As the size of the linear systems to be solved in every NRM-iteration of the semi-implicit scheme is greatly reduced in comparison with the fully-implicit scheme, we expected the semi-implicit time stepping to be a CPU cost effective

alternative to the fully-implicit approach. However, we have not observed a rapid decrease of CPU times using our implementation of the semi-implicit scheme in comparison with the fully-implicit one, not even for the eight component mixture. Nevertheless, the semi-implicit approach has some potential for parallelization, which may be investigated in future.

Another unique feature of our method is the use of the VT-flash. The main advantage of the VT-based formulation of phase equilibria over the commonly used PT-flash is that if the volume, temperature, and moles are specified, the equilibrium state of the system is uniquely determined. This is not the case for the PT-flash. We have found examples of mixtures for which equilibrium state at given pressure, temperature, and moles is not unique [11], [12], [6]. In this sense, computation of phase equilibria at specified volume, temperature, and moles is a well posed problem while the computation of the phase equilibria at specified pressure, temperature, and moles is not. The use of VT-flash also provides pressure on each element directly when the phase splitting is computed and thus in our method no artificial pressure equation (c.f. [1], [10]) has to be introduced. The direct evaluation of pressure without the need for inversion of the cubic equation of state is advantageous for pressure explicit equations of state like the Peng-Robinson equation of state. The advantage can be even higher for non-cubic equations of state like the Cubic-Plus-Association (CPA) equation of state that is important for describing the interaction of CO_2 with polar components like water. Application of this approach in CO_2 sequestration in water-containing reservoirs is another direction of our current research.

Finally, let us point out that similarly to [14], the semi-implicit scheme proposed here uses the flux approximation that does not require identification of the phases on the neighboring elements and any ad-hoc speculations on how to connect the corresponding phases on both neighboring elements. This feature is also important for CO_2 sequestration because typically, the CO_2 is injected into the reservoir in the supercritical state at which the distinction between the phases is problematic.

APPENDIX
DETAILS OF THE PENG-ROBINSON EQUATION OF STATE

We use this notation: $R = 8.314472\,\mathrm{J\,K^{-1}mol^{-1}}$ is the universal gas constant,

$$\begin{aligned} a_{ij} &= (1-\delta_{ij})\sqrt{a_i a_j}\,, \\ a_i &= 0.45724\frac{R^2\,T_{ci}^{\,2}}{p_{ci}}\left[1+m_i\left(1-\sqrt{T_{ri}}\right)\right]^2, \\ m_i &= \begin{cases} 0.37464 + 1.54226\omega_i - 0.26992\omega_i^2 \\ \qquad\qquad \text{for } \omega_i < 0.5\,, \\ 0.3796 + 1.485\omega_i - 0.1644\omega_i^2 + 0.01667\omega_i^3 \\ \qquad\qquad \text{for } \omega_i \geq 0.5\,, \end{cases} \\ T_{ri} &= \frac{T}{T_{ci}}\,, \quad b_i = 0.0778\frac{R\,T_{ci}}{p_{ci}}\,, \end{aligned} \tag{39}$$

where δ_{ij} is the binary interaction coefficient [-]; T_{ci}, p_{ci}, ω_i, T_{ri} are the critical temperature [K], critical pressure [Pa], acentric factor [-], and reduced temperature [-], respectively – all corresponding to the i-th component.

Then, pressure in (5b) is given by the Peng-Robinson equation of state [13], [5], [11], [12] as

$$\begin{aligned} &p\,(T, c_1\,, \ldots, c_{n_c}) = \\ &\quad = \frac{R\,T\sum\limits_{i=1}^{n_c} c_i}{1-\sum\limits_{i=1}^{n_c} b_i\,c_i} - \frac{\sum\limits_{i=1}^{n_c}\sum\limits_{j=1}^{n_c} a_{ij}\,c_i\,c_j}{1+2\sum\limits_{i=1}^{n_c} b_i\,c_i - \left(\sum\limits_{i=1}^{n_c} b_i\,c_i\right)^2}\,, \end{aligned} \tag{40}$$

REFERENCES

[1] G. Ács, S. Doleschall, É. Farkas. "General Purpose Compositional Model". *SPE Journal*, vol. 25, no. 4, pp 543-553, 1985 (SPE-10515-PA).

[2] F. Brezzi, M. Fortin. *Mixed and Hybrid Finite Element Methods*. Springer-Verlag, New York Inc. (1991).

[3] A. Bourgeat, M. Jurak, F. Smaï. "On persistent primary variables for numerical modeling of gas migration in a nuclear waste repository". *Computational Geosciences*, vol. 17, no. 2, pp 287-305, 2013.

[4] H. Class, R. Helmig, P. Bastian. "Numerical simulation of non-isothermal multiphase multicomponent processes in porous media.: 1. An efficient solution technique". *Advance in Water Resources*, vol. 25, no. 5, pp 533-550, 2002.

[5] A. Firoozabadi. *Thermodynamics of Hydrocarbon Reservoirs*. McGraw-Hill, NY (1998).

[6] T. Jindrová, J. Mikyška. "Fast and Robust Algorithm for Calculation of Two-Phase Equilibria at Given Volume, Temperature, and Moles". *Fluid Phase Equilibria*, vol. 353, pp 101-114, 2013, http://dx.doi.org/10.1016/j.fluid.2013.05.036.

[7] T. Jindrová, J. Mikyška. "Phase Equilibria Calculation of CO_2-H_2O System at Given Volume, Temperature, and Moles in CO_2 Sequestration". IAENG Journal of Applied Mathematics, vol. 45, no. 3, pp 183-192, 2015.

[8] R. J. Leveque. *Finite Volume Methods for Hyperbolic Problems*. Cambridge University Press, Cambridge (2002).

[9] J. Lohrenz, B. G. Bray, C. R. Clark. "Calculating Viscosities of Reservoir Fluids From Their Compositions". *Journal of Petroleum Technology*, pp 1171-1176, 1964.

[10] J. Mikyška, A. Firoozabadi. "Implementation of higher-order methods for robust and efficient compositional simulation". *Journal of Computational Physics*, vol 229, pp 2898-2913, 2010.

[11] J. Mikyška, A. Firoozabadi. "A New Thermodynamic Function for Phase-Splitting at Constant Temperature, Moles, and Volume". *AIChE Journal*, vol. 57, no.7, pp 1897-1904, 2011.

[12] J. Mikyška, A. Firoozabadi. "Investigation of Mixture Stability at Given Volume, Temperature, and Number of Moles", *Fluid Phase Equilibria*, vol. 321, pp 1-9, 2012.

[13] D. Y. Peng, D. B. Robinson. "A New Two-Constant Equation of State". *Industrial and Engineering Chemistry: Fundamentals*, vol. 15, pp 59-64, 1976.

[14] O. Polívka, J. Mikyška. "Compositional Modeling in Porous Media Using Constant Volume Flash and Flux Computation without the Need for Phase Identification". *Journal of Computational Physics*, vol. 272, pp 149-169, 2014, http://dx.doi.org/10.1016/j.jcp.2014.04.029.

[15] R. Neumann, P. Bastian, O. Ippisch. "Modeling and simulation of two-phase two-component flow with disappearing nonwetting phase". *Computational Geosciences*, vol. 17, pp 139-149, 2013.

[16] A. Quarteroni, R. Sacco, F. Saleri. *Numerical Mathematics*. Springer-Verlag, New York (2000).

[17] T. A. Davis. "A column pre-ordering strategy for the unsymmetric-pattern multifrontal method". *ACM Transactions on Mathematical Software*, vol. 30, no. 2, pp 165-195, 2004.

[18] T. A. Davis. "Algorithm 832: UMFPACK, an unsymmetric-pattern multifrontal method". *ACM Transactions on Mathematical Software*, vol. 30, no. 2, pp 196-199, 2004.

[19] T. A. Davis and I. S. Duff. "A combined unifrontal/multifrontal method for unsymmetric sparse matrices". *ACM Transactions on Mathematical Software*, vol. 25, no. 1, pp 1-19, 1999.

[20] T. A. Davis and I. S. Duff. "An unsymmetric-pattern multifrontal method for sparse LU factorization". *SIAM Journal on Matrix Analysis and Applications*, vol. 18, no. 1, pp 140-158, 1997.